HHS Public Access

Author manuscript

Cell Rep. Author manuscript; available in PMC 2016 August 31.

Published in final edited form as:

Cell Rep. 2016 August 16; 16(7): 1903–1914. doi:10.1016/j.celrep.2016.07.029.

Increased 4E-BP1 expression protects against diet-induced obesity and insulin resistance in male mice

Shih-Yin Tsai[1], **Ariana A. Rodriguez**[1], **Somasish G. Dastidar**[2], **Elizabeth Del Greco**[1], **Kaili Lia Carr**[1], **Joanna M. Sitzmann**[1], **Emmeline C. Academia**[1], **Christian Michael Viray**[1], **Lizbeth Leon Martinez**[1], **Brian Stephen Kaplowitz**[1], **Travis D. Ashe**[2], **Albert R. La Spada**[2,3,*], and **Brian K. Kennedy**[1,*]

[1]Buck Institute for Research on Aging, Novato, California, USA

[2]Department of Pediatrics, Cellular & Molecular Medicine, Department of Neurosciences, Division of Biological Sciences, Institute for Genomic Medicine, and Sanford Consortium for Regenerative Medicine, University of California, San Diego, La Jolla, California, USA

[3]Rady Children's Hospital, San Diego, California, USA

Summary

Obesity is a major risk factor driving the global type II diabetes pandemic. Yet, the molecular factors linking obesity to disease remain to be elucidated. Gender differences are apparent in humans and also observed in murine models. Here we link these differences to expression of eukaryotic translation initiation factor 4E binding protein 1 (4E-BP1), which upon HFD becomes significantly reduced in skeletal muscle and adipose tissue of male, but not female mice. Strikingly, restoring 4E-BP1 expression in male mice protects them against HFD-induced obesity and insulin resistance. Male 4E-BP1 transgenic mice also exhibit reduced white adipose tissue accumulation, accompanied by decreased circulating levels of leptin and triglycerides. Importantly, transgenic 4E-BP1 male mice are also protected from aging-induced obesity and metabolic decline on a normal diet. These results demonstrate that 4E-BP1 is a gender-specific suppressor of obesity that regulates insulin sensitivity and energy metabolism.

eTOC Blurb

Tsai et al. identify gender-specific differences in the mTOR pathway when animals are challenged with a high fat diet or during aging-related obesity. The level of one mTOR substrate, 4E-BP1,

Address correspondence to: Brian K. Kennedy, PhD, Buck Institute for Research on Aging; 8001 Redwood Blvd. Novato, CA 94945, USA. Phone: 415.209.2040; bkennedy@buckinstitute.org. Albert La Spada, MD, PhD, University of California, San Diego, 2880 Torrey Pines Scenic Drive, MC 0642, La Jolla, CA 92037, USA. Phone: 858-246-0148; alaspada@ucsd.edu.

Author Contribution

All experiments were designed and conceived by S.Y.T., A.R.L., and B.K.K. The experiments were performed by S.Y.T., A.A.R., S.G.D., J.M.S., E.C.A., and T.D.A. Data analysis was done by S.Y.T. Manuscript was written by S.Y.T., A.R.L., and B.K.K. The Lead Contact is B.K.K.

declined under these conditions in males and enhancing its levels using a transgenic approach suppresses male metabolic defects.

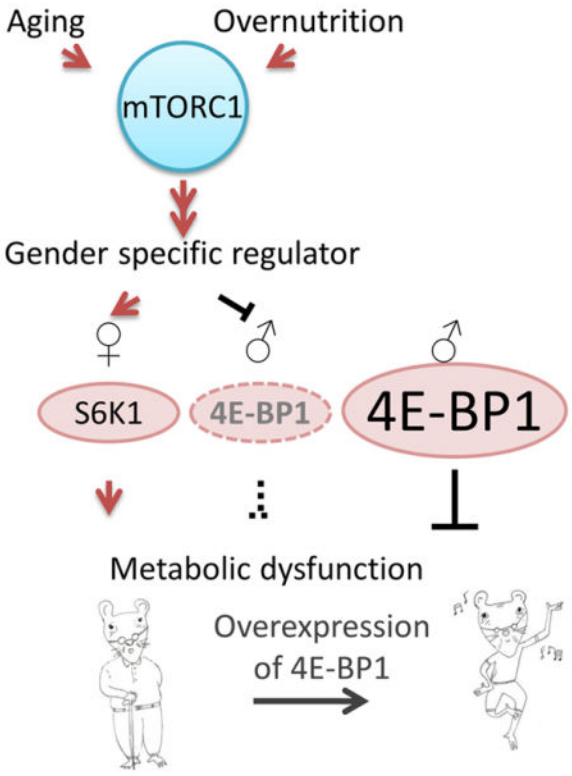

Introduction

White adipose is the major tissue that stores excess energy and regulates thermogenesis (Tseng et al., 2010; Wu et al., 2013). In addition, this tissue secretes several adipokines in the regulation of whole body metabolic homeostasis and in response to chronic inflammation, the likely cause of insulin resistance (Samuel and Shulman, 2012; Tseng et al., 2010; Zeyda and Stulnig, 2007). Obesity induced by a high fat diet (HFD) is associated with increased secretion of adipokines, such as tumor necrosis factor-α and interleukin-6, and contributes to systemic inflammation and insulin resistance. The connections between obesity, adipokine secretion and metabolic dysfunction remain to be understood.

Of individuals diagnosed with type II diabetes (T2D), nearly 80 percent are also obese. However, not all obese individuals will develop T2D (Carnethon et al., 2012; Cowie et al., 2010). Family history, age and race all contribute to individual susceptibility to T2D, suggesting that genetic factors are involved in its onset. Genetic association studies have pinpointed many risk factors (Elbein et al., 2012; Lyssenko and Laakso, 2013; Morris et al., 2012; Williams et al., 2014), but it remains poorly understood why obesity drives metabolic dysfunction in some, but not all cases.

In rodent models exposed to a HFD, gender dimorphism with respect to insulin resistance and glucose intolerance has also been reported (Grove et al., 2010; Macotela et al., 2009). A

HFD induces a similar level of obesity in male and female mice, but the level of anti-inflammatory signals are reported to be higher in female mice (Nickelson et al., 2012; Pettersson et al., 2012; Stubbins et al., 2012). This increase in anti-inflammatory signaling is correlated with maintenance of insulin sensitivity. The molecular basis for gender dimorphism is not yet fully understood.

The mammalian target of rapamycin (mTOR) kinase, a principal sensor that integrates nutrient levels to cell growth and proliferation, is a target downstream of insulin signaling (Dazert and Hall, 2011; Laplante and Sabatini, 2012). mTOR forms two functional complexes, mTOR complex 1 (mTORC1) and mTOR complex 2 (mTORC2). Activation of mTORC1 leads to the phosphorylation of the ribosomal S6 kinases (S6Ks) and 4E-BP (among other targets), which together induce ribosome biogenesis and mRNA translation (Sonenberg and Hinnebusch, 2009). mTORC1-dependent phosphorylation of 4E-BP results in dissociation of 4E-BP from eIF4E, specifically promoting cap-dependent translation initiation. Upregulation of mTORC1 signaling is often observed in tissues of obese individuals and mice, and is associated with progressive insulin resistance (Cornu et al., 2013; Laplante and Sabatini, 2012). Reduced mTORC1 activity has been reported to prevent development of T2D and protect against diabetic nephropathy in both type I and type II diabetic mouse models (Godel et al., 2011; Inoki et al., 2011; Polak et al., 2008; Um et al., 2004; Yang et al., 2007). However, the downstream target by which reduced mTORC1 activity regulates whole body metabolic homeostasis has not been determined.

Previously, 4E-BPs were shown to regulate adipogenesis and insulin sensitivity, making them strong candidates to link mTORC1 signaling and metabolism (Le Bacquer et al., 2007; Tsukiyama-Kohara et al., 2001). Whole body deletion of 4E-BP1 and 4E-BP2 yields hypersensitivity to diet-induced obesity and insulin resistance. Here, we report that gender differences in the expression of 4E-BP1 affect an individual's response to a normal- and high-fat diet. The expression of 4E-BP1 is reduced specifically in male, but not female, skeletal muscle and adipose tissues on a HFD. This loss of expression has relevance since transgenic 4E-BP1 expression protects male mice specifically from diet induced obesity and insulin resistance. Suppression of white adipose tissue accumulation is associated with reduced circulating free fatty acids, as well as the secreted hormone leptin in male 4E-BP1 transgenic mice on a HFD. Similar results were obtained in aging mice, where 4E-BP1 transgenic expression protects aging male 4E-BP1 transgenic mice from aging-induced obesity and metabolic decline. These findings reveal that a previously unappreciated gender-specific regulation of 4E-BP1 underlies differential responses to overnutrition and that maintenance of 4E-BP1 function in male mice is important to offset the detrimental metabolic consequences of obesity.

Results

Gender dimorphism in a diet-induced insulin resistance mouse model

We sought to compare and contrast the impact of a high fat diet (HFD) on obesity and metabolic dysfunction in male and female C57BL/6J mice. Mice from both genders were placed on either a normal diet (NCD) (18% calories from fat) or a HFD (60% calories from fat) for 16 weeks beginning at 8 weeks of age. During this period, HFD-fed male mice

gained 60% more weight than the NCD-fed cohort, whereas HFD-fed female mice gained 50% more weight than its NCD-fed cohort (Figure 1A). In general, males accumulated more adipose mass than females on either diet (Figure S1A), but both males and females had a similar level of obesity (approximately 38% adiposity) after 16 weeks on a HFD compared to NCD-fed mice (11% adiposity; Figure 1B).

Despite similar levels of obesity, male mice on a HFD had significantly higher fasting plasma glucose levels (Figure S1B), and developed more severe glucose intolerance and insulin resistance compared to female mice (Figure 1C and S1C). HFD-fed male mice also had markedly increased serum leptin and triglyceride levels relative to females (Figure 1D and S1D). In addition, there is a significant increase in macrophage accumulation in HFD-fed male mouse white adipose tissue (Figure 1E), which is correlated with induced pro-inflammatory gene expression (Figure 1F). Taken together, these data suggest that the intrinsic quality of adipose tissue is different in males and females on a HFD. HFD-fed male adipose tissues have enhanced secretion of factors that contribute to insulin resistance and glucose intolerance compared to adipose tissue in HFD-fed females.

Abnormal induction of mTORC1 signaling has been observed in response to insulin resistance and associated with diabetes progression (Cornu et al., 2013; Laplante and Sabatini, 2012). Thus, we examined whether the expression pattern of mTORC1 signaling downstream targets correlate with the gender dimorphism in diet-induced insulin resistance in C57BL/6J mice. Previously, upregulation of S6K1 signaling has been observed in diabetic tissues, and removal of S6K1 in mice has been reported to yield resistance to diet induced obesity and insulin resistance (Um et al., 2004). Consistent with this phenotypic observation, we found that a target of S6K1, S6, is constitutively phosphorylated in both male and female mice on a HFD (Figure S1, E and F). While S6K1 signaling is active in both genders on a HFD, the mRNA expression and protein level of 4E-BP1 was significantly reduced in HFD-fed male skeletal muscle and adipose tissues. 4E-BP1 was less affected in females with no significant difference in skeletal muscle. The basal level of 4E-BP1 expression is comparable in male and female mice on a normal diet, so the reduction of 4E-BP1 in male tissues is due to the HFD feeding (Figure 2 and S2A–E). While 4E-BP1 protein levels are comparable in female visceral fat between diets (Figure 2C and S2B), 4E-BP1 protein is highly phosphorylated in HFD-fed female visceral fat (Figure S2D–E). The levels of *4E-BP1* mRNA also become reduced in HFD-fed female adipose tissues (Figure 2A). Phosphorylation of 4E-BP1 at the mTORC1 regulated Thr37/46 site is slightly higher in HFD-fed mouse tissues (Figure S2D–E).

Next we examined possible mechanisms underlying sexual dimorphic regulation of 4E-BP1 expression. The expression of 4E-BP1 has been shown to be repressed by increased inflammatory signaling *in vitro* (Rolli-Derkinderen et al., 2003; Walsh et al., 2008; Weichhart et al., 2008). Moreover, sexual dimorphism in the inflammatory response has been reported in human obese subjects (Bloor and Symonds, 2014; Brown et al., 2010), in addition to our HFD-fed mice (Figure 1, E and F). We hypothesized that the increased inflammation upon HFD might be responsible for the decrease in 4E-BP1 expression. To test this, we treated primary mouse embryonic fibroblasts (MEFs), with an inflammatory agent, LPS, to acutely induce inflammation. Associated with the induction of pJNK signaling, 4E-

BP1 is downregulated in LPS treated MEFs (Figure S2, F and G), suggesting inflammation could be one of the factors regulating 4E-BP1 expression in diabetic tissue. This is consistent with a previous report that upregulation of the pJNK pro-inflammatory signaling pathway can repress 4E-BP1 expression in a pancreatic β cell line (Tominaga et al., 2010).

Generation and characterization of *4E-BP1* transgenic mice

Mice lacking 4E-BP1 and 4E-BP2 have increased obesity and insulin resistance on a HFD. Thus, we hypothesized that 4E-BPs are required to maintain adipose function in response to a HFD. To test this, we generated a transgenic mouse line with a conditional allele overexpressing *4EBP1*. The *4EBP1* transgenic allele (*Tg-4EBP1wt*) contains a human *4E-BP1* cDNA, which was inserted under a hybrid cytomegalovirus enhancer and chicken *β actin* promoter, and preceded by a *loxP*-flanked green fluorescent protein (GFP) with a STOP cassette (Figure S3A). *CMV-Cre* transgenic mice, which express *Cre* during early embryogenesis, were bred with *Tg-4EBP1wt* mice, to induce *4E-BP1* transgene allele expression in all tissues, including germ cells (Figure S3B). The transgenic 4E-BP1 protein competes with eIF4E associated with eIF4G from translation initiation complex as analyzed in a m^7GTP pulldown assay (Figure S3, D and E). After germ line transmission, the mice were bred to *wild-type* C57BL/6J to remove the *Cre* allele. We then back-crossed transgenic mice with whole body *4E-BP1* overexpression to the C57BL/6J background for 5 generations, to derive the *4EBP1wt-OE* mouse line for the assays described.

We found that 4E-BP1 was expressed at high levels in skeletal muscle and liver of *4EBP1wt-OE* mice with lower levels of expression in visceral fat (Figure S3B). It is also apparent that much of the expressed 4E-BP1 is in a phosphorylated state, likely as a result of mTORC1 activity (Figure S3C). *4EBP1wt-OE* mice are viable and fertile, and there is no obvious phenotype to distinguish them from control littermates (Figure S3F–H and S4, A and B). These mice also have normal glucose homeostasis, as examined in glucose tolerance and insulin challenge assays, even though male *4EBP1wt-OE* mice have a lower fasting glucose level at 6 months of age (Figure S4, A and B).

Reduced adiposity in male *4E-BP1* transgenic mice under HFD feeding

We then challenged mice with HFD feeding to see whether *4EBP1wt-OE* mice are protected from diet-induced obesity. After 16 weeks of HFD feeding, we found that male *4EBP1wt-OE* mice have a significant reduction both in body weight and adipose accumulation, while female *4EBP1-OE* mice develop a similar level of obesity as controls (Figure 3, A and B, and S4C–G). Whereas control male mice gain 60% more weight than the NCD-fed control cohort, *4EBP1wt-OE* male mice only gain 19% more weight than their NCD-fed counterparts. Moreover, male *4EBP1wt-OE* mice also show less food intake than control counterparts on a HFD (Figure S4H). The difference of weight gain in HFD-fed *4EBP1wt-OE* and control male mice is mainly attributable to less fat accumulation (Figure S4C). Consistent with reduced obesity, male *4EBP1wt-OE* mice also have lower levels of serum leptin and triglycerides compared to control mice on a HFD (Figure 3C and S4D).

Histological analysis of WT and *4EBP1wt-OE* adipose tissues clearly revealed a reduction of adiposity in male *4EBP1wt-OE* mice, with decreased white adipocyte accumulation and

reduced adipocyte size (Figure S4, E and F, and S5A). There was less accumulated white adipose tissue under the skin (subcutaneous fat) and also less white fat infiltration into brown adipose tissue, the latter consistent with modestly increased UCP1 expression in HFD-fed *4EBP1wt-OE* male mouse brown adipose tissue (Figure S4G). Moreover, there were decreased macrophage accumulation, as stained by F4/80 antigen, in male *4EBP1wt-OE* mouse visceral fat, which correlated with reduced level of IL-6 in male *4EBP1wt-OE* mouse serum (Figure S4I and S5A). Morbid obesity usually causes aberrant accumulation of triglycerides in liver, which leads to hepatic steatosis and further impairs systemic fat metabolism. However *4EBP1wt-OE* male mice, as determined by Oil red O staining, clearly demonstrated a significant reduction of accumulated triglycerides in the liver on a HFD, indicative of improved systemic fat metabolism in these mice (Figure S5A).

Maintenance of insulin sensitivity in male 4E-BP1 transgenic mice under HFD feeding

After 16 weeks of HFD feeding, both control male and female mice developed hyperglycemia. Fasting glucose was also elevated in *4EBP1wt-OE* male mice on HFD feeding, but to a lesser extent than non-transgenic control male mice (Figure 3D). Next, we examined the glucose homeostasis in *4EBP1wt-OE* mice. A glucose tolerance assay was performed to determine the ability of the mice to sense glucose elevation and secrete insulin as a means of promoting blood glucose uptake in peripheral tissues. Male *4EBP1wt-OE* mice display improved glucose homeostasis on a HFD, as demonstrated by improved glucose clearance relative to controls (Figure 3E). An insulin challenge assay was also performed to quantify systemic insulin resistance in mice on a HFD. The reduction of blood glucose levels was faster in male *4EBP1wt-OE* mice than control mice over the course of the experiment (Figure S4, K and L) with comparable insulin levels (Figure S4J). Furthermore, male *4EBP1wt-OE* mouse tissue maintained insulin-stimulated Akt phosphorylation (Figure 3F and S5C–F).

Previously, we identified increased FGF21 signaling in a different line of 4E-BP1 transgenic mice that express in skeletal muscle a 4E-BP1 mutant allele resistant to mTORC1 regulation, and demonstrated that these mice were also protected from HFD-induced obesity and insulin resistance (Tsai et al., 2015). The expression of FGF21 is also up-regulated in male *4EBP1wt-OE* mice, but this time in liver tissue (Figure S5B), suggesting the level of FGF21 and 4E-BP1 is positively associated. Another prospective mechanism in *4EBP1wt-OE* mice protected from HFD-induced metabolic dysfunction is through competing mTORC1 from activation of S6K1. However, we did not observe an alternation of phosphorylation status on either S6K1, or its target rpS6 under HFD in multiple tissues of male *4EBP1wt-OE* mice (Figure S6, A and B).

Among other mTORC1 targets examined in the HFD cohort, the phosphorylation of PRAS40, the proline-rich Akt substrate, by mTORC1 on Ser183 is increased in male mouse visceral fat upon HFD treatment (Figure S6C). Phosphorylation of PRAS40 at Ser 183 by mTORC1 has been reported to suppress its ability to inhibit mTORC1 *in vitro* (Oshiro et al., 2007; Wang et al., 2008). The level of PRAS40 phosphorylation at Ser183 was reduced in fat tissue of mice overexpressing 4E-BP1, although the trend did not reach significance (Figure S6D). The repression of PRAS40 phosphorylation in male *4EBP1wt-OE* mice is

more profound in visceral fat during aging, discussed in more detail below (Figure S9A). Previously, DEPTOR, another mTOR-interacting protein has been shown to positively regulate adipogenesis *in vitro* and its expression is associated with obesity *in vivo* (Laplante et al., 2012). The changes of DEPTOR expression were not evident in HFD-treated mouse tissues (Figure S6E), but there is a slight induction of DEPTOR expression in the visceral fat of male *4EBP1wt-OE* mice (Figure S6F). In the context of overnutrition, male *4EBP1wt-OE* mice have improved glucose tolerance and increased insulin sensitivity on a HFD. Mechanistically, the improved metabolic function might occur though induction of FGF21 production in male *4EBP1wt-OE* mice.

Tissue-specific induction of *4E-BP1* in adipose or skeletal muscle does not provide metabolic protection in mice on a HFD

Since 4E-BP1 expression is predominately reduced in adipose tissue and skeletal muscle upon HFD, we then crossed *Tg-4EBP1* mice with either *Fabp4-Cre* (*Tg-4EBP1wt;Fabp4-Cre*, refer as *Tg-4EBP1wt-fat*) or *Ckmm-Cre* (*Tg-4EBP1wt;Ckmm-Cre*, refer as *Tg-4EBP1wt-muscle*) mice to remove the *loxP*-flanked GFP-STOP codon cassette and promote *4E-BP1* transgene allele expression in mouse adipose tissue or skeletal muscle respectively (Figure S7, A and B). This approach was designed to determine whether 4E-BP1 activity is required to achieve protection from a HFD challenge. Both transgenic mouse lines were backcrossed to the C57BL/6J background for 5 generations prior to their characterization.

Both *Tg-4EBP1wt-fat* and *Tg-4EBP1wt-muscle* mice have comparable body weight, adiposity, lean body mass and glucose metabolism in comparison to control littermates (Figure 4 and S7C–E). We subjected both transgenic mouse lines to a HFD challenge starting at 8 weeks of age and monitored their weight and glucose metabolism during the course of 16 weeks. Neither *Tg-4EBP1wt-fat* nor *Tg-4EBP1wt-muscle* mice of either gender show any metabolic protection from HFD-induced obesity and insulin resistance (Figure 4 and S7C–F). The *4E-BP1* transgenic allele encodes a wildtype 4E-BP1 protein that retains regulation by mTORC1-dependent phosphorylation. Thus, increased mTORC1 signaling on a HFD may partially or fully inactivate transgenic over-expressed 4E-BP1 protein, preventing any observed metabolic protection in these transgenic mice. Consistent with this prediction, we observed an increase in 4E-BP1 phosphorylation in both transgenic mouse tissues (Figure S7, G and H). These findings suggest that the protection conferred by whole body overexpression of 4E-BP1 cannot be recapitulated by overexpression specifically in muscle or fat. The benefits must derive from expression in another tissue or a combination of tissues.

Male *4E-BP1* transgenic mice are protected from aging-induced obesity and metabolic rate decline

Both male and female *4EBP1wt-OE* mice are leaner than controls during aging, but the difference was more pronounced in male transgenic mice, which show significantly reduced adiposity starting at approximately 1 year of age (Figure 5, A and B, and S8A). Male *4EBP1wt-OE* mice also have significantly reduced levels of serum leptin and triglycerides, along with reduced adiposity (Figure S8, B and C). These differences are not the result of

altered food intake or activity (Figure S8, D and E). There is also no change in respiratory exchange ratio in *4EBP1wt-OE* mice (Figure S8F). Nevertheless, male *4EBP1wt-OE* mice have an increased metabolic rate (Figure 5, C and D), which is evident as early as 6 months of age, when their body weight is comparable to control littermates (Figure 5A). Consistent with the HFD cohort, no difference was observed in S6K1 phosphorylation, or its downstream target rpS6 (Figure S8, G and H). The protein stability of IRS1, insulin receptor substrate 1, is affected through serine phosphorylation by either S6K1 at Ser-307 or mTORC1 at Ser-636/639, and has been proposed to lead to insulin resistance (Copps and White, 2012; Um et al., 2006). Consistent with the lack of alteration of S6K1 phosphorylation, we also failed to observe any significant changes in serine phosphorylation of IRS1 or IRS1 stability (Figure S8I **and data not shown**). Moreover, there is no reduction of global translation in *4EBP1wt-OE* mouse tissues (Figure S8J).

Mice develop a comparable level of obesity during the course of a 22-month aging study and a 4-month HFD feeding study (Figure S8K). We found that there is a trend toward reduction in PRAS40 phosphorylation seen in HFD-fed *4EBP1wt-OE* male visceral fat (Figure S6D) and the reduction in PRAS40 phosphorylation is more profound during aging in the same tissue (Figure S9A).

We also observed a higher level of FGF21 (Figure S9B) in *4EBP1wt-OE* male mouse serum, likely associated with protection of brown adipose during aging (Figure S9C) and higher levels of *Ucp1* and *Pgc1α* expression in aged *4EBP1wt-OE* male brown adipose (Figure S9E). There is a slight upregulation in mRNA levels of genes involved in thermogenesis in *4EBP1wt-OE* male subcutaneous white adipose tissues (Figure S9D). Moreover, male *4EBP1wt-OE* mice have reduced muscle damage during aging, including lower numbers of centralized, vacuolated fibers and decreased intramuscular fatty acid accumulation (Figure S9, F and G).

In further analysis of aging tissues, we found a similar negative correlation of inflammation and 4E-BP1 expression as in the HFD cohort (Figure 1, E and F, and 2). The increased macrophage infiltration and induced pro-inflammatory cytokine gene expression (Figure 6, A and B) is associated with reduced 4E-BP1 expression in both aging male and female visceral fat (Figure 6C). Consistent with this notion, whole body overexpression of 4E-BP1 protected both male and female from aging-induced obesity (Figure 5, B). Moreover, there is a gender difference in expression of mTORC1 target, S6K1 and 4E-BP1 in aging tissues. 4E-BP1 is selectively reduced in male liver and visceral fat, whereas phosphorylation of S6K1, or its target S6 is exclusively up-regulated in aging female tissues (Figure 6, C and D, and S10). The distinct expression pattern of 4E-BP1 and S6K1 in aging mouse tissues could be the reason why only female *s6k1* knockout mice have lifespan extension (Selman et al., 2009) and male *4EBP1wt-OE* mice are protected from aging-induced metabolic decline.

Discussion

Here, we report a gender-dependent divergence in 4E-BP1 expression and its effect on metabolic regulation in response to different diets. With a HFD challenge, 4E-BP1 expression is significantly reduced in male skeletal muscle and adipose tissue. Male and

female mice develop a similar level of obesity on a HFD, but male mice have aggravated and deregulated lipid and glucose metabolism. Furthermore, increased expression of 4E-BP1 rescues male mice from diet-induced obesity and insulin resistance, whereas 4E-BP1 overexpression does not provide beneficial protection to HFD-fed female mice.

In the context of aging, we found that expression of 4E-BP1 is selectively downregulated in aging male mouse liver and adipose tissue. Over-expression of 4E-BP1 protects male mice from aging-induced obesity and increases energy expenditure. Conversely, we observed enhanced up-regulation of S6K1 activity in aging female liver, skeletal muscle and adipose tissues. The sexual-dimorphic regulation of two mTORC1 targets, S6K1 and 4E-BP1 correlates with the enhanced lifespan of female *s6k1* knockout mice and improved metabolic homeostasis in male *4EBP1wt-OE* mice during aging. Recently, Baar et al., reported that there is variation in mTORC1 signaling during aging of C57BL/6J mice (Baar et al., 2016). S6K1 was up-regulated in both fasted male and female adipose tissues and male skeletal muscle tissues, and there was no difference in 4E-BP1 expression reported. The differences between these two studies in the assessment of mTORC1 signaling from aging tissues could be due to the nutrition status of the mice at the time they were harvested since the mTOR pathway is highly sensitive calorie intake. We harvested mice in the morning after they had ad libitum access to food during the evening, while Baar et al., harvested mice after overnight fasting. Further studies will be required to explain how nutrition and aging intersect to influence mTOR signaling. Adipose tissue plays a central role in the management of whole body energy expenditure, regulating both glucose homeostasis and insulin sensitivity (Bluher et al., 2003). Altered mTORC1 signaling is implicated in obese human and animal adipose tissues. Specific deletion of mTORC1 in adipose tissue or whole body inactivation of its downstream mediator, S6K1 in mice, leads to reduced adiposity and increased metabolic rate. Both mice were also protected from HFD-induced obesity and insulin resistance (Polak et al., 2008; Um et al., 2004). Conversely, whole body inactivation of 4E-BP1 and 4E-BP2, which are negatively regulated by mTORC1, results in increased adiposity and sensitivity to HFD-induced metabolic dysfunction (Le Bacquer et al., 2007). Previous studies did not examine the mTORC1 pathway for gender-specific effects.

Here we have demonstrated that mTORC1 signaling behaves differently in male and female mice via 4E-BP1. A HFD preferentially suppresses 4E-BP1 expression in male adipose tissues, which is correlated with increased adiposity and adipokine secretion. Overexpression of 4E-BP1 reverses these defects. The molecular mechanism underlying how 4E-BP1 expression is differentially regulated by gender is not clear. One likely explanation involves sexual dimorphic regulation of inflammation, which in turns regulates 4E-BP1 expression.

Gender differences in the intrinsic characteristics of adipose tissue and the subsequent response to overnutrition have been reported (Macotela et al., 2009; Nickelson et al., 2012; Pettersson et al., 2012). For example, despite the higher level of body fat, female humans and rodents are more insulin-sensitive than males. During overnutrition in humans and rodents, male subjects have increased adipokine secretion, which contributes to inflammation and early abnormalities of glucose metabolism. The mechanism underlying this phenomenon in part is due to the action of estrogen and testosterone; for example,

females after menopause exhibit higher risk for the development of insulin resistance and castrated male rodents are more insulin sensitive (Mauvais-Jarvis et al., 2013). Hormonal regulation could also contribute to sex-specific regulation of 4E-BP1 expression.

It remains unclear in which tissues 4E-BP1 is regulated in a gender-specific manner during overnutrition and aging, and where overexpression of 4E-BP1 rescues metabolic dysfunction in males. Recently, we reported that transgenic expression of activated, mTORC1 non-responsive 4E-BP1 in skeletal muscle, but not adipose tissue, protects mice of both genders from high fat diet-induced metabolic dysfunction (Tsai et al., 2015). Since activated 4E-BP1 is refractory to the elevated mTORC1 signaling associated with exposure to a high fat diet, one possibility is that the primary benefits of 4E-BP1 activation is in skeletal muscle. A small increase in 4E-BP1 activity when the wild-type protein is overexpressed might only be sufficient to suppress defects associated with loss of 4E-BP1 in male mice during a high fat diet or aging. Higher skeletal muscle activity in the 4E-BP1 mutant may increase metabolic protection in both genders under the same challenges. Alternatively, the phenotypes associated with whole body overexpression of wild-type 4E-BP1 may derive from enhanced activity in other tissues. Further studies will be required to resolve this issue.

Our results demonstrate that 4E-BP1 expression in adipose and skeletal muscle tissue is a key determining factor in the gender dimorphism of fat metabolism and insulin sensitivity. In addition, they provide genetic evidence for gender differences in the response to overexpression of 4E-BP1 in obesity. Hence, our findings have important implications for the treatment of metabolic syndrome, obesity, and T2D, as gender differences in the response to drugs targeting the mTORC1 pathway may exist in humans.

Experimental Procedures

Generation of *4E-BP1* transgenic mice and Animals studies

Human *4E-BP1* cDNA was placed downstream of a *loxP*-GFP-3xstop-*loxP* cassette under the control of a chicken *β-actin* promoter. The GFP-stop cassette prevents expression of *4E-BP1* transgenic allele. Transgenic mice then were crossed with mice expressing CRE under the control of a human cytomegalovirus minimal promoter (*CMV-Cre*) to induce whole body *4E-BP1* transgenes expression, fatty acid–binding protein 4 promoter (Fabp4-Cre) to induce adipose tissue *4E-BP1* transgenes expression or the muscle creatine kinase promoter (*Ckmm-Cre*) to induce skeletal muscle tissue 4E-BP1 transgenes expression. All mice in this study are 5 generations into C57BL6/J background. In the high-fat-diet-induced type II diabetes study, mice at 8 weeks of age were placed on either a standard laboratory rodent chow (#2018, Harlan Teklad) or high-fat diet (D12492, Research Diets) as indicated and monitored for 24 weeks. Mice were handled and all *in vivo* studies were approved by the Institutional Animal Care and Use Committee (A10093) at Buck Institute for Research on Aging.

Histological analysis

Tissue samples were either fixed in 4% Paraformaldehyde solution in PBS before being embedded in paraffin or directly mounted in OCT before being stored at −80°C.

Morphology was examined in hematoxylin and eosin stained sections. The size of adipose cells were quantified in Image J. Results were shown as a mean ± SEM of independent animals 3~6. The oil red O staining was performed in OCT-mounted liver section and flash-frozen muscle tissue section. 10 μm thick sections were cut and allowed to dry for 10 minutes. After the air drying process, the slides were rinsed for a short time in distilled water and stained in 300 mg/dl oil red O solution in isopropanol for 15 min. The slides were then transferred to 60 % isopropanol to clean background and resin in distilled water, and processed for hematoxylin counter staining. Macrophage infiltration of white adipose tissue was stained using monoclonal F4/80 antibody, Invitrogen, on paraffin section.

Blood lipids, glucose and hormone analyses

Mouse blood was collected using the submandibular pouch technique. Serum was separated using serum separator tubes (BD 365956). The analysis of triglyceride, FGF21, insulin and leptin levels were performed in serum collected from mice that were fasted for 6 hours. IL-6 assay was performed on non-fasted mouse serum. The triglyceride test (2100-430) was purchased from Stanbio, the analysis of FGF21 (MF2100) and IL-6 (M6000B) ELISA was purchased from R&D, the analysis of insulin (NR 10-1247-01) ELISA was purchased from Mercodia and performed following the manufacturer's instructions. The leptin tests were done in Diabetes, endocrinology and metabolism hormone assay and analytical services core at Vanderbilt University.

Glucose and insulin tolerance assays

Glucose and insulin tolerance tests were performed on 6 month-old mice that were fasted for 6 hours. Glucose concentrations were determined with an Accu-Chek advantage glucometer (Roche) in blood collected from the tail vein at indicated time point. Insulin (0.75 U/kg for HFD group mice and 0.375 U/kg for NCD group mice) or glucose (2g/kg) was intraperitoneal injected into mice. Insulin was Humulin R (U-100) from Lilly.

RNA analyses

Total RNA was extracted from tissue using Trizol (Life technologies) following the manufacturer's instructions. (n=4 for each group; 6 month-old mice). 2 μg of total RNA was reverse transcribed into cDNA by using Superscript III reverse transcription kit (Invitrogen). Real-time PCR was performed in Roche 480 iCycler PCR machine. Reactions were performed in triplicate and relative amounts of cDNA were normalized to *Cyclophilin A* (*Ppia*). Primer sequences: *4E-BP1* Forward: CTAGCCCTACCAGCGATGAG; *4E-BP1* Reverse: CCTGGTATGAGGCCTGAATG; *Ppia* Forward: GACCAAACACAAACGGTTCC; *Ppia* Reverse: CATGCCTTCTTTCACCTTCC; *IL-6* Forward: CCGGAGAGGAGACTTCACAG; *IL-6* Reverse: TTCTGCAAGTGCATCATCGT; *Ccl-2* Forward: CCCAATGAGTAGGCTGGAGA; *Ccl-2* Reverse: TCTGGACCCATTCCTTCTTG. *Ucp-1* Forward: GCCTGGCAGATATCATCACC; *Ucp-1* Reverse: CAGACCGCTGTACAGTTTCG. *Pgc-1α* Forward: AACCACACCCACAGGATCAGA; *Pgc-1α* Reverse: TCTTCGCTTTATTGCTCCATGA; *Cidea* Forward: CTCGGCTGTCTCAATGTCAA; *Cidea* Reverse: GGAACTGTCCCGTCATCTGT; *Dio2* Forward: GCTGTGTCTGGAACAGCTTC; *Dio2* Reverse: TGAACCAAAGTTGACCACCA;

Prdm16 Forward: GAGCAGCTGAGGAAGCATTT; *Prdm16* Reverse: GCGTGGAGAGGAGTGTCTTC; *Stat6* Forward: CTGCCTAACTCAGCCTGTGG; *Stat6* Reverse: CCTGATTGCCCATAAGGAGA.

Protein isolation and immunoblotting studies

Tissues were homogenized in cold SDS lysis buffer (50mM Tris pH7.5, 70mM urea, 250mM sucrose and 2% SDS) with protease inhibitor cocktail (Roche 04693124001) and phosphatase inhibitor cocktail II and III (Sigma P5726 and P0044). Total proteins were separated in 4–12% Invitrogen BT precast gel (NP0315) or any KD Bio-rad TGX precast gel (456–9033) and transferred to Nitrocellulose membranes. Antibodies were from Cell Signaling (α-4E-BP1(#9252), α-phospho-4EBP1 Ser 65 (#9451), α-phospho-4EBP1 Thr 37/46 (#9459), α-S6 (#2217), α-phospho-S6 Ser 235/236 (#2211), α-AKT1 (#4691), α-phospho-AKT Ser 473 (#4060), α-JNK (#9258), α-phospho-JNK Thr183/Tyr185 (#9251), α-eIF4E (#2067), α-eIF4G (#2469), α-S6K1 (#2708), α-phospho-S6K1 Thr 389 (#9234), α-PRAS40 (#2691), α-phospho-PRAS40 Ser 183 (#5936), α-IRS1 (#3015), α-phospho-IRS1 Ser 636/639 (#2388), α-HSP90 (#4877), α-αtubulin (#3873) and α-β ACTIN (#4967)), abcam (α-FGF21 (ab171941), and α-UCP1 (ab23841)), and EMD Millipore (α-DEPTOR, ABS222)

Indirect calorimetric studies

Oxygen consumption, CO_2 production, home activity, and food were measured by open-flow respirometry (Sable systems, USA).

Statistics

Unless otherwise stated, all results are expressed as means ± SEM of n observations. Statistical differences between the means were assessed by a two-way ANOVA and all the glucose tolerance assays and insulin challenge assays were analyzed by a two-way ANOVA for repeated measures. Bonferroni post-tests to compare replicate means by row.

Supplementary Material

Refer to Web version on PubMed Central for supplementary material.

Acknowledgments

This study was supported by NIH Grants R01AG033373 and R01AG035336 to B.K.K. and R01 AG033082 to A.R.L. B.K.K. is also an Ellison Medical Foundation Senior Scholar in Aging. Graphic Abstract was contributed by Wan-Lin Lo.

References

Baar EL, Carbajal KA, Ong IM, Lamming DW. Sex- and tissue-specific changes in mTOR signaling with age in C57BL/6J mice. Aging Cell. 2016; 15:155–166. [PubMed: 26695882]

Bloor ID, Symonds ME. Sexual dimorphism in white and brown adipose tissue with obesity and inflammation. Horm Behav. 2014; 66:95–103. [PubMed: 24589990]

Bluher M, Kahn BB, Kahn CR. Extended longevity in mice lacking the insulin receptor in adipose tissue. Science. 2003; 299:572–574. [PubMed: 12543978]

Brown LM, Gent L, Davis K, Clegg DJ. Metabolic impact of sex hormones on obesity. Brain Res. 2010; 1350:77–85. [PubMed: 20441773]

Carnethon MR, De Chavez PJ, Biggs ML, Lewis CE, Pankow JS, Bertoni AG, Golden SH, Liu K, Mukamal KJ, Campbell-Jenkins B, et al. Association of weight status with mortality in adults with incident diabetes. JAMA. 2012; 308:581–590. [PubMed: 22871870]

Copps KD, White MF. Regulation of insulin sensitivity by serine/threonine phosphorylation of insulin receptor substrate proteins IRS1 and IRS2. Diabetologia. 2012; 55:2565–2582. [PubMed: 22869320]

Cornu M, Albert V, Hall MN. mTOR in aging, metabolism, and cancer. Curr Opin Genet Dev. 2013; 23:53–62. [PubMed: 23317514]

Cowie CC, Rust KF, Byrd-Holt DD, Gregg EW, Ford ES, Geiss LS, Bainbridge KE, Fradkin JE. Prevalence of diabetes and high risk for diabetes using A1C criteria in the U.S. population in 1988–2006. Diabetes Care. 2010; 33:562–568. [PubMed: 20067953]

Dazert E, Hall MN. mTOR signaling in disease. Curr Opin Cell Biol. 2011; 23:744–755. [PubMed: 21963299]

Elbein SC, Gamazon ER, Das SK, Rasouli N, Kern PA, Cox NJ. Genetic risk factors for type 2 diabetes: a trans-regulatory genetic architecture? Am J Hum Genet. 2012; 91:466–477. [PubMed: 22958899]

Godel M, Hartleben B, Herbach N, Liu S, Zschiedrich S, Lu S, Debreczeni-Mor A, Lindenmeyer MT, Rastaldi MP, Hartleben G, et al. Role of mTOR in podocyte function and diabetic nephropathy in humans and mice. J Clin Invest. 2011; 121:2197–2209. [PubMed: 21606591]

Grove KL, Fried SK, Greenberg AS, Xiao XQ, Clegg DJ. A microarray analysis of sexual dimorphism of adipose tissues in high-fat-diet-induced obese mice. Int J Obes (Lond). 2010; 34:989–1000. [PubMed: 20157318]

Inoki K, Mori H, Wang J, Suzuki T, Hong S, Yoshida S, Blattner SM, Ikenoue T, Ruegg MA, Hall MN, et al. mTORC1 activation in podocytes is a critical step in the development of diabetic nephropathy in mice. J Clin Invest. 2011; 121:2181–2196. [PubMed: 21606597]

Laplante M, Horvat S, Festuccia WT, Birsoy K, Prevorsek Z, Efeyan A, Sabatini DM. DEPTOR cell-autonomously promotes adipogenesis, and its expression is associated with obesity. Cell Metab. 2012; 16:202–212. [PubMed: 22883231]

Laplante M, Sabatini DM. mTOR signaling in growth control and disease. Cell. 2012; 149:274–293. [PubMed: 22500797]

Le Bacquer O, Petroulakis E, Paglialunga S, Poulin F, Richard D, Cianflone K, Sonenberg N. Elevated sensitivity to diet-induced obesity and insulin resistance in mice lacking 4E-BP1 and 4E-BP2. J Clin Invest. 2007; 117:387–396. [PubMed: 17273556]

Lyssenko V, Laakso M. Genetic screening for the risk of type 2 diabetes: worthless or valuable? Diabetes Care. 2013; 36(Suppl 2):S120–126. [PubMed: 23882036]

Macotela Y, Boucher J, Tran TT, Kahn CR. Sex and depot differences in adipocyte insulin sensitivity and glucose metabolism. Diabetes. 2009; 58:803–812. [PubMed: 19136652]

Mauvais-Jarvis F, Clegg DJ, Hevener AL. The role of estrogens in control of energy balance and glucose homeostasis. Endocr Rev. 2013; 34:309–338. [PubMed: 23460719]

Morris AP, Voight BF, Teslovich TM, Ferreira T, Segre AV, Steinthorsdottir V, Strawbridge RJ, Khan H, Grallert H, Mahajan A, et al. Large-scale association analysis provides insights into the genetic architecture and pathophysiology of type 2 diabetes. Nat Genet. 2012; 44:981–990. [PubMed: 22885922]

Nickelson KJ, Stromsdorfer KL, Pickering RT, Liu TW, Ortinau LC, Keating AF, Perfield JW 2nd. A comparison of inflammatory and oxidative stress markers in adipose tissue from weight-matched obese male and female mice. Exp Diabetes Res. 2012; 2012:859395. [PubMed: 22778716]

Pettersson US, Walden TB, Carlsson PO, Jansson L, Phillipson M. Female mice are protected against high-fat diet induced metabolic syndrome and increase the regulatory T cell population in adipose tissue. PLoS One. 2012; 7:e46057. [PubMed: 23049932]

Polak P, Cybulski N, Feige JN, Auwerx J, Ruegg MA, Hall MN. Adipose-specific knockout of raptor results in lean mice with enhanced mitochondrial respiration. Cell Metab. 2008; 8:399–410. [PubMed: 19046571]

Rolli-Derkinderen M, Machavoine F, Baraban JM, Grolleau A, Beretta L, Dy M. ERK and p38 inhibit the expression of 4E-BP1 repressor of translation through induction of Egr-1. J Biol Chem. 2003; 278:18859–18867. [PubMed: 12618431]

Samuel VT, Shulman GI. Mechanisms for insulin resistance: common threads and missing links. Cell. 2012; 148:852–871. [PubMed: 22385956]

Selman C, Tullet JM, Wieser D, Irvine E, Lingard SJ, Choudhury AI, Claret M, Al-Qassab H, Carmignac D, Ramadani F, et al. Ribosomal protein S6 kinase 1 signaling regulates mammalian life span. Science. 2009; 326:140–144. [PubMed: 19797661]

Sonenberg N, Hinnebusch AG. Regulation of translation initiation in eukaryotes: mechanisms and biological targets. Cell. 2009; 136:731–745. [PubMed: 19239892]

Stubbins RE, Najjar K, Holcomb VB, Hong J, Nunez NP. Oestrogen alters adipocyte biology and protects female mice from adipocyte inflammation and insulin resistance. Diabetes Obes Metab. 2012; 14:58–66. [PubMed: 21834845]

Tominaga R, Yamaguchi S, Satake C, Usui M, Tanji Y, Kondo K, Katagiri H, Oka Y, Ishihara H. The JNK pathway modulates expression and phosphorylation of 4E-BP1 in MIN6 pancreatic beta-cells under oxidative stress conditions. Cell Biochem Funct. 2010; 28:387–393. [PubMed: 20589738]

Tsai S, Sitzmann JM, Dastidar SG, Rodriguez AA, Vu SL, McDonald CE, Academia EC, O'Leary MN, Ashe TD, La Spada AR, et al. Muscle-specific 4E-BP1 signaling activation improves metabolic parameters during aging and obesity. J Clin Invest. 2015; 125:2952–2964. [PubMed: 26121750]

Tseng YH, Cypess AM, Kahn CR. Cellular bioenergetics as a target for obesity therapy. Nat Rev Drug Discov. 2010; 9:465–482. [PubMed: 20514071]

Tsukiyama-Kohara K, Poulin F, Kohara M, DeMaria CT, Cheng A, Wu Z, Gingras AC, Katsume A, Elchebly M, Spiegelman BM, et al. Adipose tissue reduction in mice lacking the translational inhibitor 4E-BP1. Nat Med. 2001; 7:1128–1132. [PubMed: 11590436]

Um SH, D'Alessio D, Thomas G. Nutrient overload, insulin resistance, and ribosomal protein S6 kinase 1, S6K1. Cell Metab. 2006; 3:393–402. [PubMed: 16753575]

Um SH, Frigerio F, Watanabe M, Picard F, Joaquin M, Sticker M, Fumagalli S, Allegrini PR, Kozma SC, Auwerx J, et al. Absence of S6K1 protects against age- and diet-induced obesity while enhancing insulin sensitivity. Nature. 2004; 431:200–205. [PubMed: 15306821]

Walsh D, Arias C, Perez C, Halladin D, Escandon M, Ueda T, Watanabe-Fukunaga R, Fukunaga R, Mohr I. Eukaryotic translation initiation factor 4F architectural alterations accompany translation initiation factor redistribution in poxvirus-infected cells. Mol Cell Biol. 2008; 28:2648–2658. [PubMed: 18250159]

Weichhart T, Costantino G, Poglitsch M, Rosner M, Zeyda M, Stuhlmeier KM, Kolbe T, Stulnig TM, Horl WH, Hengstschlager M, et al. The TSC-mTOR signaling pathway regulates the innate inflammatory response. Immunity. 2008; 29:565–577. [PubMed: 18848473]

Williams AL, Jacobs SB, Moreno-Macias H, Huerta-Chagoya A, Churchhouse C, Marquez-Luna C, Garcia-Ortiz H, Gomez-Vazquez MJ, Burtt NP, Aguilar-Salinas CA, et al. Sequence variants in SLC16A11 are a common risk factor for type 2 diabetes in Mexico. Nature. 2014; 506:97–101. [PubMed: 24390345]

Wu J, Cohen P, Spiegelman BM. Adaptive thermogenesis in adipocytes: is beige the new brown? Genes Dev. 2013; 27:234–250. [PubMed: 23388824]

Yang Y, Wang J, Qin L, Shou Z, Zhao J, Wang H, Chen Y, Chen J. Rapamycin prevents early steps of the development of diabetic nephropathy in rats. Am J Nephrol. 2007; 27:495–502. [PubMed: 17671379]

Zeyda M, Stulnig TM. Adipose tissue macrophages. Immunol Lett. 2007; 112:61–67. [PubMed: 17719095]

Highlights

1. Gender differences in expression of 4E-BP1 upon overnutrition.
2. 4E-BP1 is a gender-specific suppressor of metabolic dysfunction.
3. Transgenic 4E-BP1 male mice are protected from age-induced metabolic dysfunction.

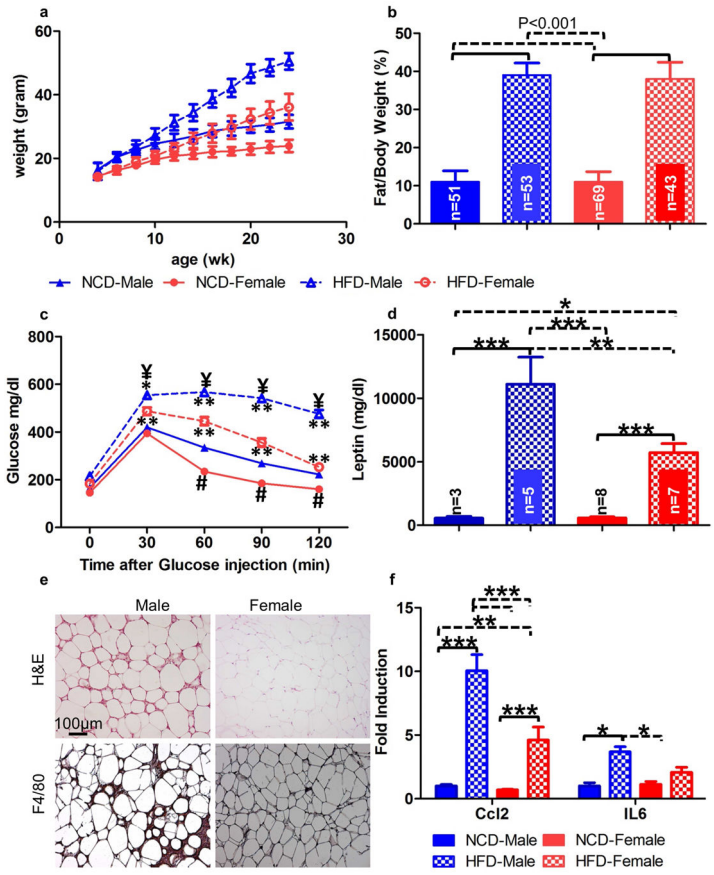

Figure 1. Gender dimorphism in diet-induced insulin resistance and glucose intolerance in C57BL/6J mouse strain

A. Body weight measurement in *wild-type* C57BL/6J male and female mice on a normal chow and HFD (n=20–53). P<0.001[NCD vs HFD: Male started at 10 wk. and Female started at wk.12]. P<0.001[male vs female: NCD started at wk.4]. P<0.001[male vs female: HFD started at wk.6].

B. Fat mass measurement normalized with body weight in 6-month-old *wild-type* C57BL/6J male and female mice on a normal chow and HFD.

C. Glucose tolerance assay in 6-hr-fasting *wild-type* C57BL/6J male and female mice on a normal chow and HFD (n=36–44). *P<0.05;**P<0.001[NCD vs HFD: same gender]. #P<0.001[male vs female: NCD]. ¥P<0.001[male vs female: HFD].

D. Plasma leptin measurement in 6-month-old *wild-type* C57BL/6J male and female mice on a normal chow and HFD. P value of the cross comparison from the other groups was labeled *P<0.05;**P<0.01; ***P<0.001.

E. Hematoxylin & Eosin (top) and F4/80 IHC (bottom) staining of the visceral fat from 6-month-old HFD-fed *wildtype* male and female mice (n= 4~7 for each group).

F. Real-time PCR analysis of proinflammatory gene expression in visceral fat from 6-month-old normal-diet-fed or HFD-fed male or female mice (n=4). Fold induction was normalized to female normal-diet-fed samples. P value of the cross comparison from the other groups was labeled *P<0.05;**P<0.01; ***P<0.001.

All graphs are plotted as means ± SEM of n, number of mice used in each analysis. Number of samples analyzed indicated in figure. P values were calculated by a two-way ANOVA [(B), (D), and (F)], and a two-way ANOVA for repeated measures [(A) and (C)] with Bonferroni post-tests to compare replicate means by row.

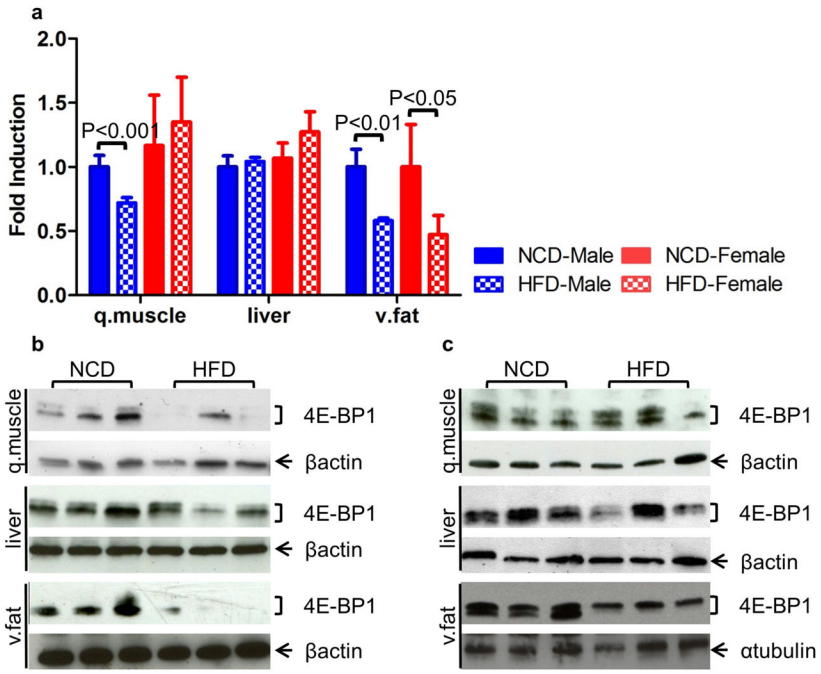

Figure 2. Differential 4E-BP1 expression in 6-month-old C57BL/6J mouse strain on a HFD

A. Real-time PCR analysis of *4E-BP1* mRNA expression in quadriceps muscle, liver and visceral fat from normal-diet-fed and HFD-fed male and female mice (n=4). Fold induction was normalized to male normal-diet-fed samples. Results are presented as means ± SEM. P values were calculated by a two-way ANOVA with Bonferroni post-tests to compare replicate means by row.

B. Western blot of 4E-BP1 protein expression in quadriceps muscle, liver and visceral fat from normal-diet-fed or HFD-fed male mice.

C. Western blot of 4E-BP1 protein expression in quadriceps muscle, liver and visceral fat from normal-diet-fed or HFD-fed female mice.

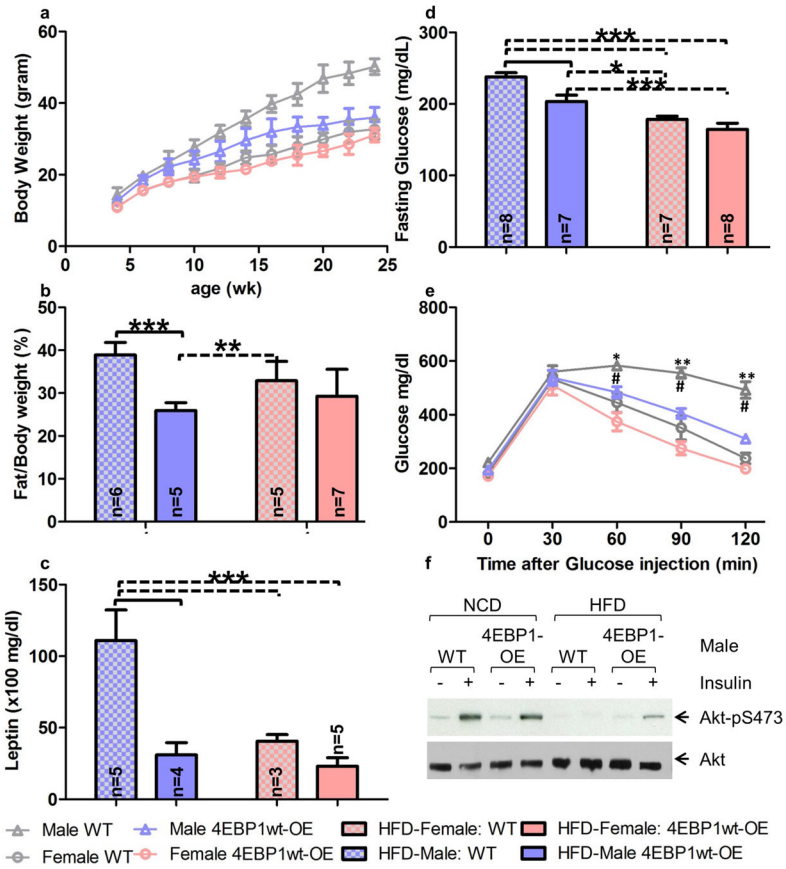

Figure 3. Male *4EBP1-OE* transgenic mice protect from diet induced obesity and maintain insulin sensitivity

A. Body weight measurement in *4EBP1-OE* transgenic and *wild-type* mice on a HFD (n=7–9). P<0.001[WT vs *4EBP1-OE*: Male started at wk.10]. P<0.001[male vs female: WT started at wk. 8]. P<0.001[male vs female: *4EBP1-OE* started at 8 wk.]. [male *4EBP1-OE* vs female WT, P<0.01 at wk.8–14, P<0.001 at wk.16–18 and P<0.05 at wk.20]. P<0.001[male WT vs female *4EBP1-OE* started at wk. 6].

B. Adiposity measurement in 6-month-old *4EBP1-OE* transgenic and *wild-type* mice on a HFD.

C. Plasma leptin measurement in *4EBP1-OE* transgenic and *wild-type* mice on a HFD at 6 month-old of age.

D. Plasma glucose measurement in 6-hr-fasting *4EBP1-OE* transgenic and *wild-type* mice on a HFD at 6 month-old of age.

E. Glucose tolerance assay in 6-hr-fasting *4EBP1-OE* transgenic and *wild-type* mice on a HFD at 6 month-old of age (n=9). *P<0.05; **P<0.001 [*WT* vs *4EBP1wt-OE*: male]. #P<0.001 [male vs female: WT].

F. Western blot of phosphorylation of AKT1 at Ser 473 and total AKT1 protein expression in visceral fat of *4EBP1-OE* transgenic and *wild-type* male mice before (−) or after (+) insulin stimulation on a normal chow or HFD at 6 month-old of age.

All graphs are plotted as means ± SEM of n, number of mice used in each analysis. Number of samples analyzed indicated in figure. P values were calculated by a two-way ANOVA

[(B), (C), and (D)] and a two-way ANOVA for repeated measures [(A) and (E)] with Bonferroni post-tests to compare replicate means by row. For simplicity, Figure (B), (C), and (D), P value of the cross comparison from the other groups was labeled *P<0.05;**P<0.01; ***P<0.001.

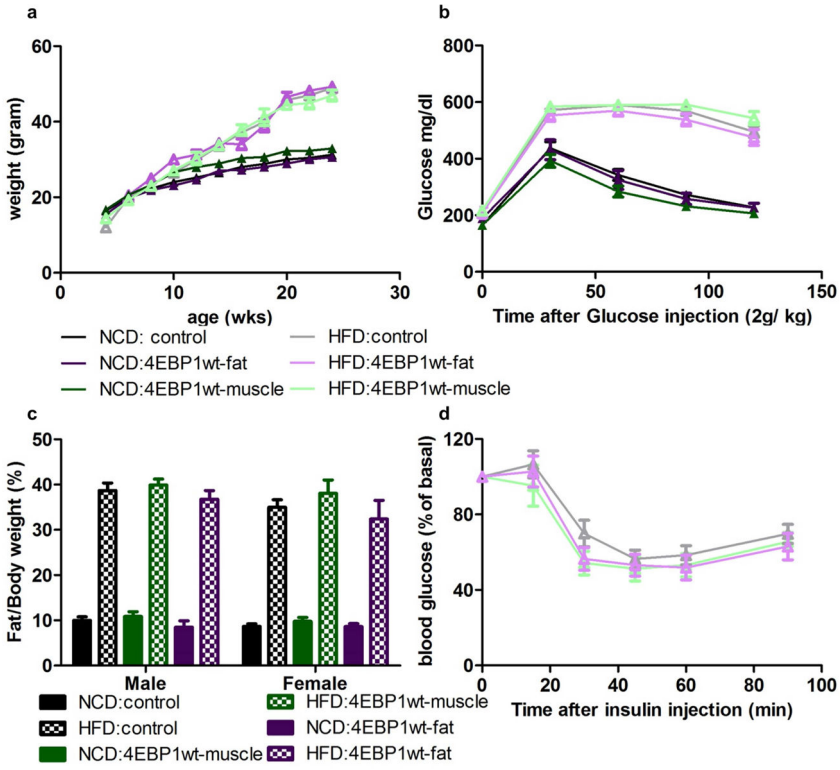

Figure 4. Assessment of metabolic parameter in *4E-BP1* double transgenic male mice

A. Body weight measurement in *Tg-4EBP1wt-fat* and *Tg-4EBp1wt-muscle* male mice on a normal chow and HFD (n=8–16). P<0.001[NCD vs HFD: Male started at 10 wk.]

B. Glucose tolerance assay in 6-hr-fasting *Tg-4EBP1wt-fat* and *Tg-4EBp1wt-muscle* male mice on a normal chow and HFD at 6 month-old of age (n=8–16). P<0.001[NCD vs HFD in all genetic group comparison: Male started at 30 min. time point]

C. Fat mass measurement normalized with body weight in *Tg-4EBP1wt-fat* and *Tg-4EBp1wt-muscle* mice on a normal chow and HFD at 6 month-old of age (n=8–16). P<0.001[NCD vs HFD in all genetic and gender group comparison]

D. Insulin challenge assay in 6-hr-fasting *Tg-4EBP1wt-fat* and *Tg-4EBp1wt-muscle* male mice on a HFD at 6 month-old of age (n=8–16).

All graphs are plotted as means ± SEM of n, number of mice used in each analysis. Number of samples analyzed indicated in figure. P values were calculated by a two-way ANOVA [(C)] and a two-way ANOVA for repeated measures [(B) and (D)] with Bonferroni post-tests to compare replicate means by row.

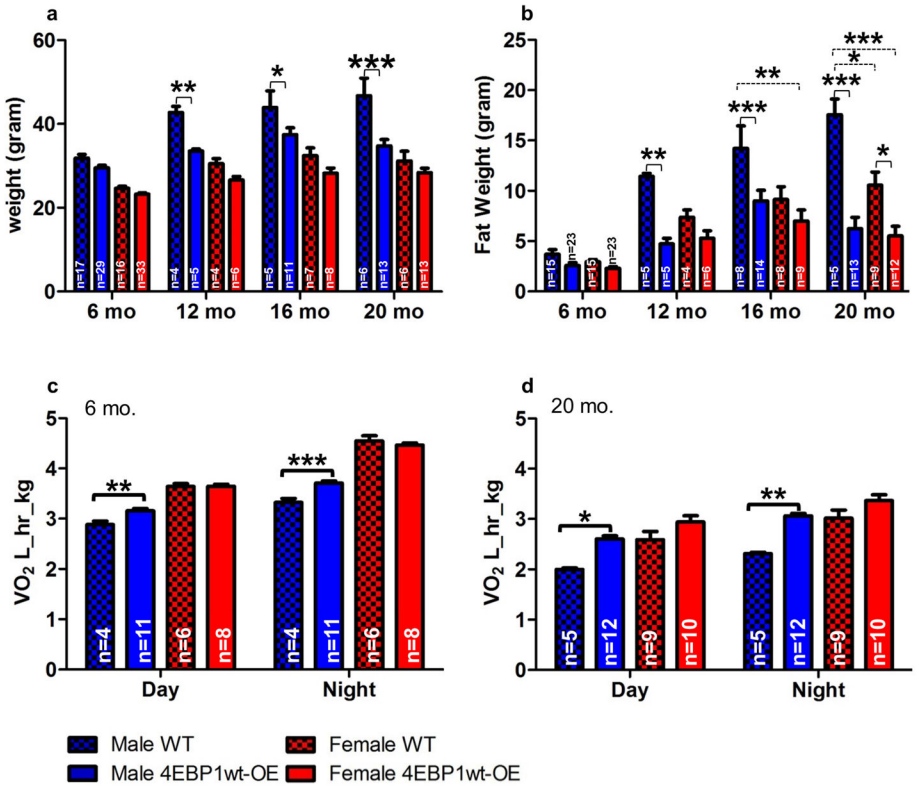

Figure 5. Metabolic parameters of aging *4EBP1-OE* transgenic and *wild-type* mice under a normal chow

a. Body weight measurement in *4EBP1-OE* transgenic and *wild-type* mice on a normal chow. P<0.001[male vs female: WT]. P<0.001[male vs female: *4EBP1-OE*]. [male *4EBP1-OE* vs female WT, P<0.01 at 6 mo.]. P<0.001 [male WT vs female *4EBP1-OE*].

b. Fat weight measurement in *4EBP1-OE* transgenic and *wild-type* mice on a normal chow during aging.

c. Oxygen consumption in *4EBP1-OE* transgenic and *wild-type* mice on a normal chow at 6 month of age. P<0.001[male vs female: WT], P<0.001 [male WT vs female *4EBP1-OE*], P<0.001[male *4EBP1-OE* vs female], P<0.001 [male WT vs female *4EBP1-OE*].

d. Oxygen consumption in *4EBP1-OE* transgenic and *wild-type* mice on a normal chow at 20 month of age. P<0.01[male vs female: WT], P<0.001 [male WT vs female *4EBP1-OE*].

All graphs are plotted as means ± SEM of n, number of mice used in each analysis. Number of samples analyzed indicated in figure. P values were calculated by a two-way ANOVA with Bonferroni post-tests to compare replicate means by row. *P<0.05;**P<0.01; ***P<0.001

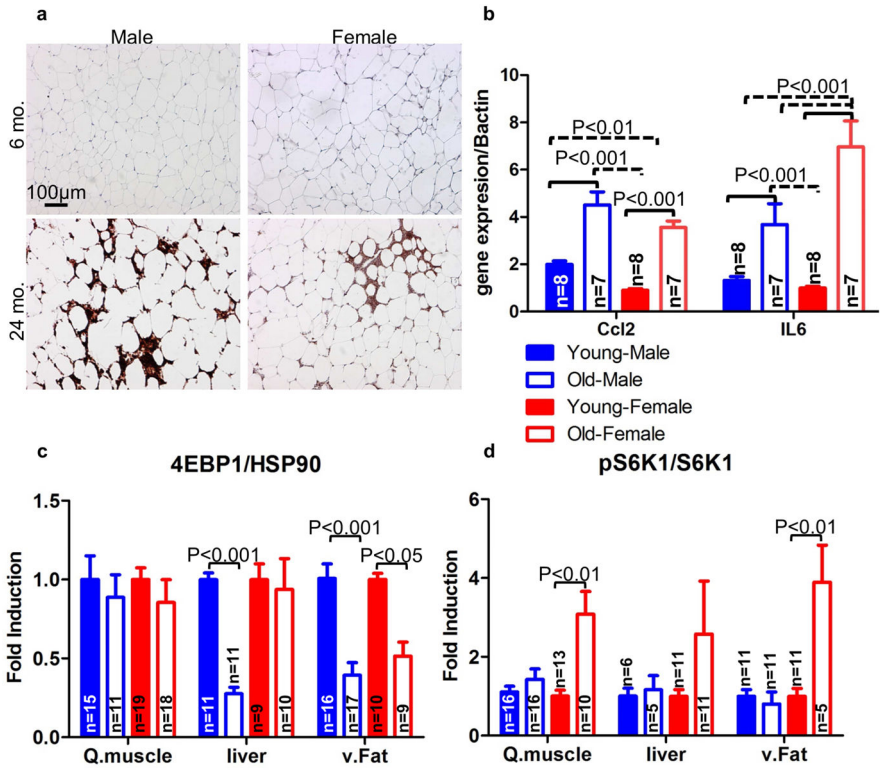

Figure 6. Gender dimorphism in expression of 4E-BP1 and activity of S6K1 in aging C57BL/6J mouse strain

A. Macrophage infiltration in the visceral fat stained by F4/80 IHC from 6-month-old or 24-month-old *wild-type* male and female mice. (n=4 for 6-month old cohort and n=7 for 24-month old cohort).

B. Real-time PCR analysis of proinflammatory gene expression in visceral fat from 6-month-old or 24-month-old *wild-type* male or female mice (n=8 for 6-month old cohort and n=7 for 24-month old cohort). Fold induction was normalized to 6-month-old female samples.

C. Quantification of western blot of 4E-BP1expression normalized with housekeeping gene, HSP90, relative to 6-month-old samples.

D. Quantification of western blot of phosphorylated S6K1 at Thr 389 normalized with total S6K1 expression, relative to 6-month-old samples.

Young mouse cohort are from 6-month-of-old mice and old mouse cohort are from 24-month-old mice. All graphs are plotted as means ± SEM of n, number of mice used in each analysis. P values were calculated by a two-way ANOVA with Bonferroni post-tests to compare replicate means by row.